Available online at www.sciencedirect.com
ScienceDirect
Bioorganic & Medicinal Chemistry 16 (2008) 4466–4470
Bioorganic & Medicinal Chemistry

Identification of neomycin B-binding site in T box antiterminator model RNA

Rajaneesh Anupam,[a,b] Leyna Denapoli,[a] Abigael Muchenditsi[a] and Jennifer V. Hines[a,b,*]

[a]*Department of Chemistry and Biochemistry, Ohio University, Athens, OH 45701, USA*
[b]*Molecular and Cellular Biology Program, Ohio University, Athens, OH 45701, USA*

Received 29 October 2007; revised 12 February 2008; accepted 19 February 2008
Available online 7 March 2008

Abstract—The T box transcription antitermination mechanism regulates the expression of unique genes in many Gram-positive bacteria by responding, in a magnesium-dependent manner, to uncharged cognate tRNA base pairing with an antiterminator RNA element and other regions of the 5′-untranslated region. Model T box antiterminator RNA is known to bind aminoglycosides, ligands that typically bind RNA in divalent metal ion-binding sites. In this study, enzymatic footprinting and spectroscopic assays were used to identify and characterize the binding site of neomycin B to an antiterminator model RNA. Neomycin B binds the antiterminator bulge nucleotides in an electrostatic-dependent manner and displaces 3–4 monovalent cations, indicating that the antiterminator likely contains a divalent metal ion-binding site. Neomycin B facilitates rather than inhibits tRNA binding indicating that bulge-targeted inhibitors that bind the antiterminator via non-electrostatic interactions may be the more optimal candidates for antiterminator-targeted ligand design.

1. Introduction

The T box genes are regulated by a common transcription antitermination mechanism.[1–3] This mechanism is used in the regulation of many tRNA synthetase, amino acid biosynthetic, and amino acid transport genes of Gram-positive bacteria.[4] With several hundred examples identified[5,6] and the biological importance of the genes regulated by the T box mechanism, it is an intriguing potential target for investigating small molecule-induced disruption. The 5′ untranslated region (5′UTR) of the T box family of genes is characterized by conserved primary and secondary structural elements, the most conserved of which is the 14-nucleotide region called the T box.[7,8] The formation of two alternative secondary structural elements, terminator and antiterminator, in this region controls the expression of the gene. The formation of the terminator halts transcription whereas the formation of the antiterminator allows the transcription of the complete gene message. The antiterminator, containing the T box sequence, is thermodynamically less stable than the terminator,[5] but is stabilized by base pairing with the acceptor end nucleotides of cognate uncharged tRNA.[1] This base pairing occurs with the first four bases at the 5′ end of a seven nucleotide bulge in the antiterminator and is critical for effecting antitermination.[9] The anticodon of the uncharged cognate tRNA also base pairs with a codon-like sequence in the 'specifier loop' of stem 1, a structurally conserved region at the beginning of the 5′UTR.[2,3] This base pairing provides the cognate specificity to the T box antitermination mechanism.[1] While the binding of tRNA to the 5′UTR occurs in the absence of additional cofactors,[10,11] antitermination requires a minimum threshold of divalent metal ion (15 mM Mg^{2+}).[12]

Mechanistically, the most intriguing interaction in this T box riboswitch is the binding of the tRNA acceptor end to the antiterminator. Functionally relevant model systems have been developed to better characterize the molecular details of this interaction and to explore the design of antiterminator-targeted small molecule inhibitors.[11] Recently, we reported that aminoglycosides bind the T box antiterminator RNA with neomycin B having the highest affinity (K_d = 8 μM).[13] While the affinity is weaker than some high-affinity aminoglycoside–rRNA complexes,[14] it is comparable to other specific aminoglycoside–RNA complexes.[15] The fluorescence resonance

Keywords: Aminoglycoside; RNA; Antitermination; T box; Binding; Inhibition.
* Corresponding author. Tel.: +1 740 593 1737; fax: +1 740 517 8482; e-mail: hinesj@ohio.edu

0968-0896/$ - see front matter © 2008 Elsevier Ltd. All rights reserved.
doi:10.1016/j.bmc.2008.02.056

energy transfer (FRET)-binding assays indicated that neomycin B altered the bend angle between the two helices of the antiterminator, strongly indicating that the binding site might be in the bulge region of the antiterminator. Given the antitermination requirement for divalent metal ion[12] and the propensity for aminoglycosides to bind in divalent metal ion-binding sites,[16,17] it is possible that the antiterminator contains a divalent metal ion-binding site. Ionic effects on affinity and enzymatic probing were carried out in order to investigate how neomycin B binds the antiterminator. The information gained from these studies is important for a better understanding of the T box antitermination mechanism and for future ligand design for antiterminator-targeted disruption of this biologically important riboswitch.

2. Results

2.1. Identification of neomycin-binding site

Enzymatic footprinting was used to locate the specific-binding site of neomycin B. The addition of neomycin B to AM1A (Fig. 1A) resulted in changes in the RNase A cleavage patterns (Fig. 1B). The most significant protection occurred at nucleotides 6–8, located in the bulge of the antiterminator model RNA and to a lesser extent, C22.

Enzymatic probing results with RNase T1, an alternative single-strand specific RNase, showed neomycin-induced protection in similar regions of the antiterminator as was observed with RNase A (nucleotides 7–10) along with G2–G3 in helix A1. There was also a slight enhancement of enzymatic cleavage in the middle of helix A2 at G15.

2.2. Structural effects of neomycin binding

Circular dichroism was used to monitor the possible secondary structural effects of neomycin B binding to antiterminator model RNA AM1A. In the presence of increasing concentrations of neomycin B (0–200 μm), there is only a slight shift (2 nm at 200 μm neomycin B) to longer wavelengths in the region of 235–260 nm (Fig. 2A). There are no significant differences in the maximal molar elipticity observed at either 209 nm or 268 nm (regions affected by significant changes in phosphate backbone and base stacking, respectively).

2.3. Ionic effects on neomycin–antiterminator affinity

The binding of neomycin B to AM1A was monitored in the presence of varying concentrations of monovalent cation to investigate ionic effects. Using methods derived from a FRET AM1A-binding assay,[13] the K_d values for neomycin B-binding 3′-Fl-18-Rh-AM1A were determined for five different concentrations ranging from 55 to 100 mM Na^+. The replicate data were analyzed similar to that described previously.[13] A linear analysis of the $-\log K_a$ versus log [Na^+] plot (Fig. 2B) resulted in a slope = 2.6 ± 0.5.

2.4. Neomycin effects on tRNA–antiterminator affinity

Binding studies in the presence of an excess of neomycin B were conducted to determine if neomycin B disrupted cognate tRNA-UCCA[18] (Fig. 3A) binding to the antiterminator. The large excess of neomycin B (200 μM, 25 times the FRET-derived[13] K_d value of 8 μM) was used to ensure complete saturation of the antiterminator neomycin B-binding site. It is important to note that while neomycin B induced changes in the FRET of the di-fluorescently labeled antiterminator model (attributed to altering the bend angle between helix A1 and A2[13]), neomycin B induced no significant change in the fluorescence when added to mono labeled 5′-Fl-AM1A alone (0–200 μM neomycin B titration data not shown and Fig. 3B). The tRNA-binding isotherms in the presence and absence of neomycin B were determined using a previously reported method.[18]

The presence of neomycin B (200 μM) enhanced the fluorescence of the antiterminator–tRNA complex approximately twofold (Fig. 3B), but did not significantly alter the K_d value for tRNA binding the antiterminator (Fig. 3C, $K_d = 0.3 \pm 0.2$ μM with neomycin B versus $K_d = 0.1 \pm 0.05$ μM without neomycin B).

3. Discussion

Aminoglycoside ligands have been extensively studied for their ability to bind RNA.[19,20] This class of compounds binds a variety of RNA targets including the 16S rRNA,[21] HIV viral RNA[22] and ribozymes.[23] The aminoglycosides are believed to bind RNA at two different types of sites. The first type consists of a helical domain with a widened major groove while the second type consists of a complex metal ion-containing pocket.[24] In previous FRET monitored ligand-binding studies, aminoglycosides were found to bind antiterminator model RNA in a structurally specific manner based on the core structure of the aminoglycoside.[13] In addition, the affinity increased with increasing number of nitrogens indicating that electrostatics played a significant role in binding. Since the solution structure of the antiterminator model RNA AM1A had characteristics of both types of aminoglycoside-binding sites (a deformed helical structure in stem A2 and bulge nucleotides that formed, along with the stems, an extra-helical pocket),[25] we undertook to definitively identify and characterize the neomycin B-binding site in AM1A. The neomycin-induced FRET change previously observed in the aminoglycoside-binding assays was attributed to a change in the bend angle between helix A1 and A2 most likely from neomycin binding in the bulge region.[13] However, changes in the FRET would also be expected if neomycin bound helix A2 and further deformed the helical structure of this region. The binding site of neomycin B was characterized to distinguish between these two possibilities in order to gain better insight into the system for future antiterminator-targeted small molecule inhibition of T box transcription antitermination.

The enzymatic cleavage assays localized the neomycin-binding site to the 5′ end of the antiterminator bulge

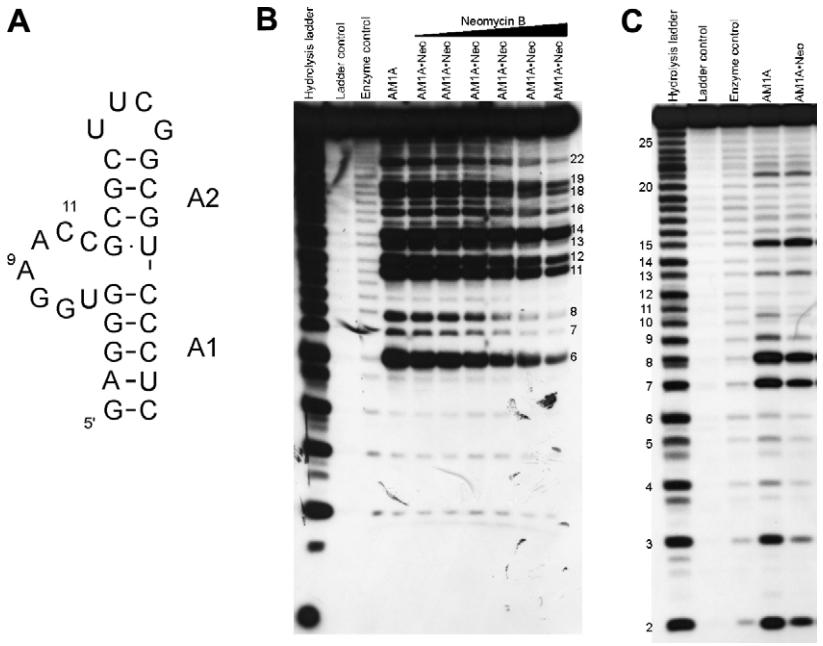

Figure 1. (A) Antiterminator model RNA AM1A. (B) RNase A footprinting of AM1A and AM1A–neomycin B complex. Lane 1, alkaline hydrolysis ladder; lane 2, hydrolysis control; lane 3, RNase A control; lane 4, AM1A; lanes 5–10, AM1A with increasing concentrations of neomycin B (10, 20, 40, 80, 100, and 200 μM). (C) RNase T1 footprinting of AM1A and AM1A–neomycin B complex. Lane 1, alkaline hydrolysis ladder; lane 2, hydrolysis control; lane 3, RNase T1 control; lane 4, AM1A; lane 5, AM1A with neomycin B (100 μM).

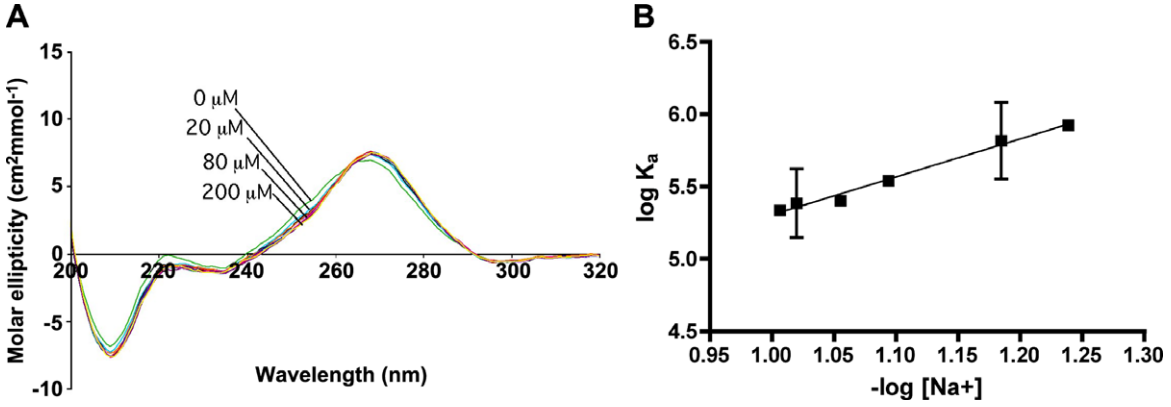

Figure 2. (A) Circular dichroism spectrum of AM1A with increasing concentration of neomycin B ranging from 0 to 200 μM in 20 μM increments. (B) Salt dependence of neomycin B binding to AM1A.

since this is the region where the greatest protection in the presence of neomycin was observed for both enzymes. There were only minimal changes in enzymatic cleavage in helix A2. The data indicate that it is not likely that neomycin B is binding in the helix A2 region, but rather that binding in the bulge leads to a slight change in helix A2 (e.g., slight enhancement of RNase T1 cleavage at G15). This is consistent with the unrestrained molecular dynamics studies of randomly docked neomycin–antiterminator RNA complexes where neomycin also localized at the 5′ end of the bulge (R. Anupam, J. Hines, unpublished results). The CD spectra of AM1A indicated that there was no significant change in the stacking of the antiterminator RNA secondary structure upon addition of neomycin B, but there were changes to the phosphate backbone. The data support the initial hypothesis that neomycin B binds the bulge nucleotides leading to a small structural change in helix A2 and possibly a change in the bend angle between the two helices.

The ionic strength dependence of binding was analyzed using polyelectrolyte theory[26] as has been used to analyze other aminoglycoside–RNA interactions.[15] The slope of the $\log K_a$ versus $-\log[Na^+]$ plot is equal to $m\Psi$, where m is the number of ions displaced from the nucleic acid by the ligand and Ψ is the fractional probability that a counterion is thermodynamically associated with each phosphate group on the nucleic acid (estimates range from 0.68 to 0.89).[27] In the case of neomycin B-binding AM1A, the slope of the ionic effect on K_a plot (Fig. 2B) was 2.6 ± 0.5, indicating that 3–4 monovalent cations are displaced by neomycin B upon binding to the antiterminator model. Other aminoglyco-

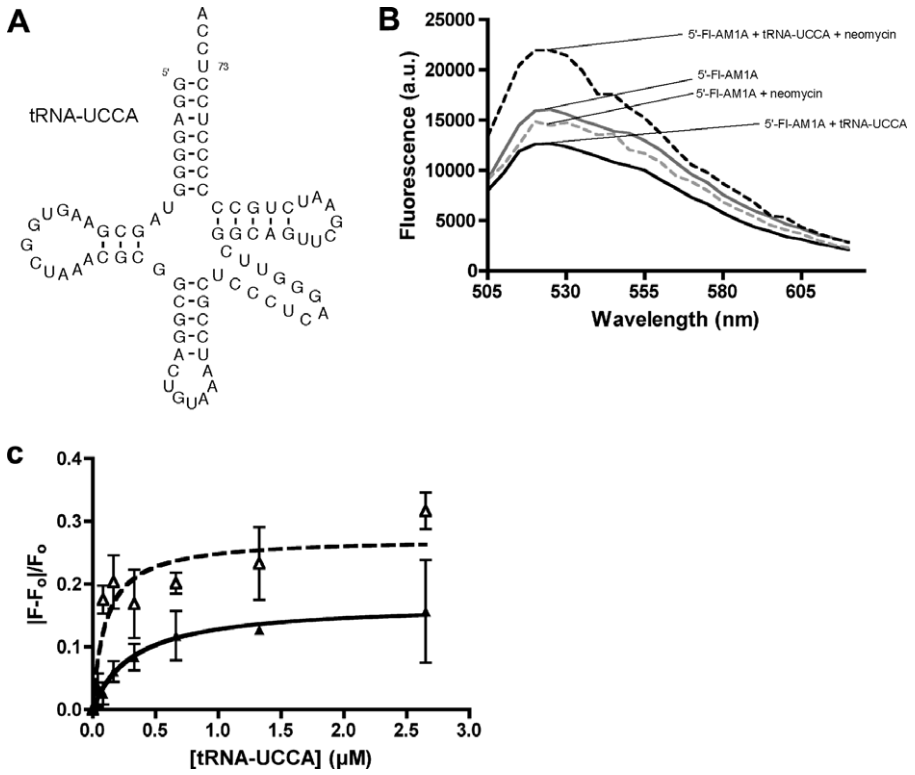

Figure 3. (A) Secondary structure of cognate tRNA-UCCA. (B) Fluorescence emission spectra of 5′-Fl-AM1A (100 nM) in the presence of neomycin B (200 μM) or tRNA-UCCA (1 μM) or both as indicated. (C) Binding of tRNA-UCCA to AM1A in the absence (dashed line, open triangles) and in the presence (solid line, solid triangle) of neomycin B (200 μM).

side–RNA complexes result in displacement of a similar number of monovalent cations.[28] Since aminoglycosides typically bind in divalent metal ion-binding sties (of both high and moderate affinity),[16,17] the data indicate that a divalent metal ion-binding site may exist in the bulge region of the antiterminator. This is consistent with in vitro transcription antitermination results where a high concentration of Mg^{2+} was not required for the tRNA anticodon to bind the T box leader at the 'specifier sequence', but was required to effect antitermination, thus implying that the tRNA acceptor end binding to the antiterminator is affected by the Mg^{2+}.[12,29] The divalent cation may structurally organize the antiterminator to facilitate-binding tRNA.

Due to the ability of aminoglycosides to inhibit other RNA processes,[30] the effect of neomycin B on formation of the tRNA–antiterminator RNA complex was investigated. There was no significant change in the affinity for tRNA-binding antiterminator RNA. Instead, based on the dramatic change in the fluorescence of the tRNA–antiterminator–neomycin complex compared to the tRNA–antiterminator complex, there was a structural change in the tRNA–antiterminator complex induced by neomycin B. Even with the large excess of neomycin B used in the disruption assay, it is reasonable that neomycin B did not inhibit the tRNA binding given the significantly higher affinity of tRNA for AM1A[18] compared to that of neomycin B for AM1A.[13] In addition, the change in the fluorescence of the tRNA–antiterminator complex in the presence of neomycin indicates that a new aminoglycoside-binding site is forming in the context of the complex.

4. Conclusions

The specific localization of the neomycin B-binding site to the 5′ end of the bulge in T box antiterminator RNA indicates that a ligand-binding pocket is formed by the bulge nucleotides that may also be a divalent metal ion-binding site. Significantly, while electrostatic interactions enhance ligand affinity, electrostatic attraction alone, in the vicinity of the antiterminator nucleotides that base pair with the tRNA, is not sufficient to inhibit tRNA binding. Consequently, a focus on bulge-targeted ligands that bind the antiterminator via non-electrostatic interactions is likely the best approach for future antiterminator-targeted ligand design.

5. Experimental

5.1. RNA preparation

The AM1A and tRNA-UCCA were synthesized from DNA templates using T7 polymerase.[31,32] The single-stranded template for AM1A was obtained from Integrated DNA Technologies, Inc. The DNA template for tRNA-UCCA was PCR amplified from a plasmid construct.[33] All RNAs were gel purified on 20% denaturing polyacrylamide (19:1 acrylamide/bisacrylamide)

gels. Fluorescently labeled RNAs were obtained from Dharmacon, Inc. All RNAs were dialyzed against 10 mM sodium phosphate, pH 6.5, 0.01 mM EDTA prior to use.

5.2. Enzymatic footprinting

AM1A was ^{32}P 5′ end-labeled using Kinase Max (Ambion). Each footprinting reaction (10 μl) consisted of 10 mM Tris buffer, pH 7, 100 mM KCl, 10 mM $MgCl_2$, 250 nM of labeled AM1A, and 3 μg of yeast RNA. Neomycin B was added to each reaction mixture as indicated in Figure 1. The labeled AM1A was pre-incubated with neomycin B for 15 min at room temperature. The reaction was then incubated with 0.01 U of RNase A or RNase T1 for 15 min and the reaction stopped by adding an equal volume of gel loading buffer containing 8 M urea. The reaction was resolved on 20 % denaturing polyacrylamide gel (19:1 acrylamide/bisacrylamide), visualized using autoradiography and the band intensities were measured using *Bio-Rad Quantity One v.4*. Each band was normalized by the total intensities of its respective lane.

5.3. Circular dichroism

The CD spectra (200–300 nm) were acquired on a JASCO model J-715 spectrometer at 4 °C in 50 mM sodium phosphate, pH 6.5, 5 mM $MgCl_2$, 50 mM NaCl, 0.01 mM EDTA. Aliquots (2 μl) of neomycin B were added to 100 μl of 10 μM AM1A in 20 μM increments from 0 to 200 μM final concentration of neomycin B. Similar addition of neomycin B to 100 μl of buffer with no RNA present resulted in no change in the CD spectrum (data not shown).

5.4. Salt-dependence neomycin-binding assays (3′-Fl-18-Rh-AM1A monitored binding)

The labeled material and general procedure were the same as those used previously for monitoring aminoglycoside binding to FRET-labeled AM1A.[13] Each K_d value was determined from the average of replicate-binding isotherms at a set total Na^+ concentration. Individual-binding mixtures (100 μl) for each isotherm consisted of NaCl (fixed amount of 5–50 mM), 50 mM sodium phosphate buffer, pH 6.5, 5 mM Mg^{2+} and 0.01 mM EDTA and neomycin B ranging from 0 to 14 mM with 100 nM 3′-Fl-18-Rh-AM1A. The FRET was measured and the K_d determined as previously described.[13]

5.5. tRNA-binding assays (5′-Fl-AM1A monitored binding)

The labeled material and general procedure were similar to those previously described for monitoring tRNA binding to 5′-Fl-AM1A.[18] Assays involved a set of serial dilutions of tRNA-UCCA with 5′-Fl-AM1A (100 nM) in 50 mM sodium phosphate, pH 6.5, 0.01 mM EDTA, 50 mM NaCl, 5 mM $MgCl_2$, with or without 200 μM of neomycin B at 25 °C. The relative normalized fluorescence was measured after incubation (60 min) and the K_d determined as previously described.[18]

Acknowledgments

This work was supported in part by the National Institutes of Health (GM61048); Ohio Super Computing Center; and, the Office of the Vice President for Research, Ohio University.

References and notes

1. Grundy, F. J.; Henkin, T. M. *Cell* **1993**, *74*, 475.
2. Grundy, F. J.; Henkin, T. M. *Curr. Opin. Microbiol.* **2004**, *7*, 126.
3. Henkin, T. M.; Grundy, F. J. *Cold Spring Harbor Symp. Quant. Biol.* **2006**, *71*, 1.
4. Henkin, T. M. *Mol. Microbiol.* **1994**, *13*, 381.
5. Grundy, F. J.; Moir, T. R.; Haldeman, M. T.; Henkin, T. M. *Nucleic Acids Res.* **2002**, *30*, 1646.
6. Panina, E. M.; Vitreschak, A. G.; Mironov, A. A.; Gelfand, M. S. *FEMS Microbiol. Lett.* **2003**, *222*, 211.
7. Henkin, T. M.; Glass, B. L.; Grundy, F. J. *J. Bacteriol.* **1992**, *174*, 1299.
8. Grundy, F. J.; Henkin, T. M. *J. Mol. Biol.* **1994**, *235*, 798.
9. Grundy, F. J.; Rollins, S. M.; Henkin, T. M. *J. Bacteriol.* **1994**, *176*, 4518.
10. Grundy, F. J.; Winkler, W. C.; Henkin, T. M. *Proc. Natl. Acad. Sci. U.S.A.* **2002**, *99*, 11121.
11. Gerdeman, M. S.; Henkin, T. M.; Hines, J. V. *Nucleic Acids Res.* **2002**, *30*, 1065.
12. Yousef, M. R.; Grundy, F. J.; Henkin, T. M. *J. Mol. Biol.* **2005**, *349*, 273.
13. Means, J. A.; Hines, J. V. *Bioorg. Med. Chem. Lett.* **2005**, *15*, 2169.
14. Fourmy, D.; Recht, M. I.; Puglisi, J. D. *J. Mol. Biol.* **1998**, *277*, 347.
15. Blount, K. F.; Tor, Y. *Nucleic Acids Res.* **2003**, *31*, 5490.
16. Hermann, T.; Westhof, E. *J. Mol. Biol.* **1998**, *276*, 903.
17. Mikkelsen, N. E.; Johansson, K.; Virtanen, A.; Kirsebom, L. A. *Nat. Struct. Biol.* **2001**, *8*, 510.
18. Means, J. A.; Wolf, S.; Agyeman, A.; Burton, J. S.; Simson, C. M.; Hines, J. V. *Chem. Biol. Drug Des.* **2007**, *69*, 139.
19. Tor, Y. *Chembiochem* **2003**, *4*, 998.
20. Vicens, Q.; Westhof, E. *Chembiochem* **2003**, *4*, 1018.
21. Moazed, D.; Noller, H. F. *Nature* **1987**, *327*, 389.
22. Zapp, M. L.; Stern, S.; Green, M. R. *Cell* **1993**, *74*, 969.
23. Vonahsen, U.; Davies, J.; Schroeder, R. *Nature* **1991**, *353*, 368.
24. Schroeder, R.; Waldsich, C.; Wank, H. *EMBO J.* **2000**, *19*, 1.
25. Gerdeman, M. S.; Henkin, T. M.; Hines, J. V. *J. Mol. Biol.* **2003**, *326*, 189.
26. Lohman, T. M.; deHaseth, P. L.; Record, M. T., Jr. *Biochemistry* **1980**, *19*, 3522.
27. Record, M. T., Jr; Anderson, C. F.; Lohman, T. M. *Q. Rev. Biophys.* **1978**, *11*, 103.
28. Kaul, M.; Pilch, D. *Biochemistry* **2002**, *41*, 7695.
29. Grundy, F. J.; Yousef, M. R.; Henkin, T. M. *J. Mol. Biol.* **2005**, *346*, 73.
30. Zaman, G. J. R.; Michiels, P. J. A.; van Boeckel, C. A. A. *Drug Discovery Today* **2003**, *8*, 297.
31. Milligan, J. F.; Uhlenbeck, O. C. *Methods Enzymol.* **1989**, *180*, 51.
32. Milligan, J. F.; Groebe, D. R.; Witherell, G. W.; Uhlenbeck, O. C. *Nucleic Acids Res.* **1987**, *15*, 8783.
33. Fauzi, H.; Jack, K. D.; Hines, J. V. *Nucleic Acids Res.* **2005**, *33*, 2595.